Kinematics of X-Y Pedestals with Joint and Pointing Misalignment

Buğra Coşkun*†

Profen Communication
Technologies & Services, Inc.

26.11.2023

Abstract

We describe the kinematics of X-Y pedestals with unideal geometry caused by joint and pointing misalignment that might arise from issues in manufacturing, assembly or mechanical wear. We present it's real and complex inverse kinematic solutions that are produced through classical methods of analysis and test their validity using simulations of discrete rotations.

Introduction

X-Y pedestals are manipulators of two revolute joints ideally positioned orthogonally with one stacked on top of the other, with both parallel to the tangent plane of Earth spheroid at that location. They are a popular design choice for low-earth-orbit satellite tracking applications of high-elevation passes. They are preferred over the alternative altitude-azimuth pedestals that suffer the zenith problem at positions closer to the azimuth singularity [1]. While all serial manipulators have singularities [2], For X-Y pedestals the singularity is located at the axis of the stationary joint. This is a concern only for low elevation applications which is a rare occurence for satellite communications[3]. X-Y pedestal kinematics is not as intuitive as their altitude-azimuth counterpart, but given their popularity previous research delving into their dynamics, kinematics and control that lessens this property already exists[4]. In this paper we hope to fill the gap for a more general inverse kinematics solution that considers pedestals with misalignment issues without the need for resynthesizing the inverse kinematics solution.

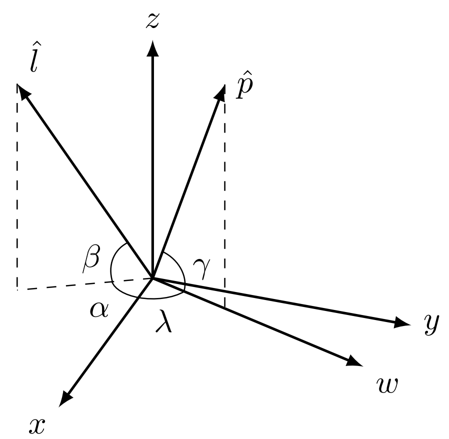

Figure 1: Pedestal coordinate system with exagerated misalignments

For the mathematical model; the stationary joint axis will be deemed the X-joint and will coincide with $\hat{x}$ in the pedestal standard basis and it's rotation angle shall be expressed as ψ. For $\psi = 0$ the Y-joint axis will be $\hat{w}$ at an angle λ with $\hat{x}$ and let ϕ be it's rotation angle. $\hat{w}$ will belong to the same plane defined by the vectors $\hat{x}$ and $\hat{y}$. As such the joint misalignment is $\frac{\pi}{2} - \lambda$. Let $\hat{p}$ be the orientation vector at $\psi = 0$ and $\phi = 0$. Similar to joint misalignment, pointing misalignment is $\frac{\pi}{2} - \gamma$. In a real-world case the pedestal basis should be defined in the NWU or NED frame so as to meet these definitions. This involves calculating the pedestal $\hat{z}$ from positions of pedestal $\hat{x}$ and $\hat{w}$ vectors in the selected environment frame and produce a rotation matrix. This will make it so that any joint misalignment can be considered using the

*E-mail: bugra.coskun@profen.com

†ORCID: 0009-0002-0177-684X

definitions above. Let the target orientation be $\hat{l}$. For inverse kinematics this is usually given as azimuth and elevation angles and in left-handed spherical coordinates. Taking the negative of the azimuth angle gives us α and we can produce the cartesian vector using the appropriate spherical to cartesian mapping.

Forward Kinematics

We first consider the rotation around the Y-joint, as Y-joint axis is modified by the X-joint rotation, this will save us from calculating the new axis of the Y-joint. This is an example of extrinsic rotation.

$$\hat{w} = \begin{bmatrix} \cos\lambda \\ \sin\lambda \\ 0 \end{bmatrix}, \tag{1}$$

The skew-symmetric cross product matrix of $\hat{w}$ is therefore:

$$W = \begin{bmatrix} 0 & 0 & \sin\lambda \\ 0 & 0 & -\cos\lambda \\ -\sin\lambda & \cos\lambda & 0 \end{bmatrix}, \tag{2}$$

The rotation matrix for Y-joint in $SO(3)$ group is given by the Rodrigues' rotation formula:

$$R_{\hat{w}}(\phi) = I + (\sin\phi)W + (1-\cos\phi)W^2, \tag{3}$$

The elementary rotation matrix around the $\hat{x}$ axis is in the form:

$$R_x(\psi) = \begin{bmatrix} 1 & 0 & 0 \\ 0 & \cos\psi & -\sin\psi \\ 0 & \sin\psi & \cos\psi \end{bmatrix}, \tag{4}$$

We define the orientation vector at initial configuration $\psi = 0$ and $\phi = 0$ to be:

$$\hat{p} = \begin{bmatrix} \cos\lambda\cos\gamma \\ \sin\lambda\cos\gamma \\ \sin\gamma \end{bmatrix}, \tag{5}$$

Thus the forward kinematic equation becomes:

$$\hat{l} = R_{\hat{x}}(\psi)R_{\hat{w}}(\phi)\hat{p}. \tag{6}$$

The resulting line-of-sight vector is in the pedestal frame, which ideally shall coincide with the North-West-Up frame for our model. Any tilt in the pedestal frame can be accounted for if we know the orientation of the pedestal and produce the rotation matrix that gives us the position of pedestal basis in the NWU frame similar to gimbal calculations for stabilizing the line of sight[5].

Inverse Kinematics

For inverse kinematics we introduce the concepts of joint surface and loose reachability. We define the surface of a joint as being the set of all unitary vectors where their dot products against the joint axis are some value c.

$$c \in (-1,1),\ \mathbb{S}_{\hat{k}}(c) = \{\hat{v} : \hat{v}\cdot\hat{k} = c\}. \tag{7}$$

For any rotation around the joint axis the dot products of vectors belonging to the surface are conserved:

$$\begin{gathered} \forall\hat{v} \in \mathbb{S}_{\hat{k}}(c),\ \forall\theta \in (-\pi,\pi], \\ R_{\hat{k}}(\theta)\hat{v} \in \mathbb{S}_{\hat{k}}(c) \because R_{\hat{k}}(\theta) \in SO(3). \end{gathered} \tag{8}$$

Following that,

$$\hat{l} \in \mathbb{S}_{\hat{x}}(\hat{l}\cdot\hat{x}) \ \therefore R_{\hat{x}}(\psi)R_{\hat{w}}(\phi)\hat{p} = \hat{l} \tag{9}$$

$$\iff R_{\hat{w}}(\phi)\hat{p} \in \mathbb{S}_{\hat{x}}(\hat{l}\cdot\hat{x}) \tag{10}$$

$$\iff R_{\hat{w}}(\phi)\hat{p}\cdot\hat{x} = \hat{l}\cdot\hat{x}. \tag{11}$$

Thus if $\exists\phi \in (-\pi,\pi]$ such that Eq(9) holds we consider the position to be loosely reachable (ie. a real solution exists without considering joint limitations). Solving Eq(10) for ϕ we get:

$$\phi = \sin^{-1}\left[\frac{\cos\alpha\cos\beta - \cos\gamma\cos\lambda}{\sin\gamma\sin\lambda}\right]. \tag{12}$$

If the position is not loosely reachable and $sin^{-1}(x)$ is extended into the complex plane so that it's defined for $||x|| > 1$ then $\mathrm{Im}(\phi) \neq 0$. In such a case the complex angles can be used to find the closest approximate position in the workspace [6].

For solving X-Joint angle ψ independently from the ϕ angle we leverage the fact that $\hat{p}^*$ shall belong to both joint surfaces if a proper ϕ angle exists,

$$\hat{p}^* = R_{\hat{w}}(\phi)\hat{p}, \tag{13}$$

$$\hat{p}^* \in \mathbb{S}_{\hat{x}}(\hat{l}\cdot\hat{x}) \cap \mathbb{S}_{\hat{w}}(\hat{p}\cdot\hat{w}), \tag{14}$$

Using this this property we construct the equation that shall consider ψ in isolation from ϕ,

$$R_{\hat{x}}(\psi)\hat{p}^* = \hat{l} \iff \hat{p}^* = R_{\hat{x}}^{-1}(\psi)\hat{l} \tag{15}$$

$$\iff R_{\hat{x}}(-\psi)\hat{l} \in \mathbb{S}_{\hat{w}}(\hat{p}\cdot\hat{w}) \tag{16}$$

$$\iff R_{\hat{x}}(-\psi)\hat{l}\cdot\hat{w} = \hat{p}\cdot\hat{w}, \tag{17}$$

From Eq(15) we get the transcendental equation:

$$\begin{aligned}\cos\psi\sin\alpha\cos\beta\sin\lambda + \sin\psi\sin\beta\sin\lambda \\ - \cos\alpha\cos\beta\cos\lambda + \cos\gamma = 0,\end{aligned} \tag{18}$$

To solve this we employ Euler's formula and consider ψ in the complex plane. With some algebraic manipulation and application of the quadratic formula we receive the equation for the nearest root:

$$\psi = i\log\left(\frac{\begin{array}{l}-(\cos^2\alpha\cos^2\beta \\ -2\cos\alpha\cos\beta\cos\gamma\cos\lambda \\ +\cos^2\gamma+\cos^2\lambda-1)^{\frac{1}{2}} \\ +\cos\alpha\cos\beta\cos\lambda-\cos\gamma\end{array}}{(\sin\alpha\cos\beta - i\sin\beta)\sin\lambda}\right). \tag{19}$$

Alternatively (as in some computational cases it may be undesirable to use complex numbers), through vector analysis we can compare $\hat{l}$ and $\hat{p}^*$ in the plane defined by $\hat{x}$ using their cross products with $\hat{x}$ and synthesize another ψ equation that way. Incidentally we do not need to project $\hat{l}$ and $\hat{p}^*$ entirely, their rotation angle around the joint axis will be preserved for their cross product with the joint axis.

$$\forall c \in (-1,1),\ \forall\hat{k};\ \forall\hat{v},\forall\hat{u} \in \mathbb{S}_{\hat{k}}(c), \tag{20}$$

$$R_{\hat{k}}(\theta)\hat{v} = \hat{u} \iff R_{\hat{k}}(\theta)(\hat{v}\times\hat{k}) = (\hat{u}\times\hat{k}) \tag{21}$$

It is clear that the resulting vector from the cross product of normalized $\hat{p}^* \times \hat{x}$ and $\hat{p}^* \times \hat{x}$ vectors will be parallel to $\hat{x}$. And will be equivalent if the rotation angle is positive and vice versa. To find the sign of the angle in left-handed rotation around $\hat{x}$ we use the dot product. Thus the vector equation and it's simplified trigonometric form are constructed as such:

$$\begin{aligned}\psi &= \sin^{-1}\left[\left(\frac{\hat{p}^*\times\hat{x}}{||\hat{p}^*\times\hat{x}||}\times\frac{\hat{l}\times\hat{x}}{||\hat{l}\times\hat{x}||}\right)\cdot\hat{x}\right], \\ &= \sin^{-1}\left(\frac{\begin{array}{l}-(\sin\gamma\sin\phi\cos\lambda \\ \quad -\sin\lambda\cos\gamma)\sin\beta \\ \quad\quad +\sin\alpha\sin\gamma\cos\beta\cos\phi\end{array}}{\begin{array}{l}(-\cos^2\alpha\cos^2\beta+1)^{\frac{1}{2}} \\ \quad [(\sin\gamma\sin\phi\cos\lambda \\ \quad\quad -\sin\lambda\cos\gamma)^2 \\ \quad\quad\quad +\sin^2\gamma\cos^2\phi]^{\frac{1}{2}}\end{array}}\right).\end{aligned} \tag{22}$$

Simulation of Discrete Rotations

To verify the produced equations we test their output by comparing the result of rotations acting on $\hat{p}$ to the target orientation $\hat{l}$. To visualize the process further we rotate $\hat{p}$ around $\hat{w}$ first to produce $\hat{p}^*$ and then apply the rotation around $\hat{x}$.

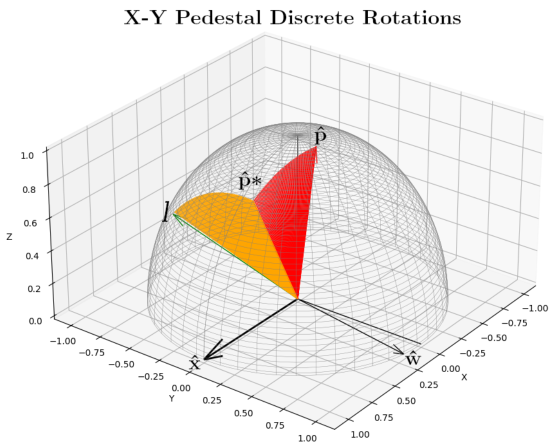

Figure 2: Simulation of discrete rotations with produced angles

For the simulation in Figure 2, we apply the parameters $\alpha = \frac{\pi}{4.5}$, $\beta = \frac{\pi}{4}$, $\lambda = \frac{\pi}{2.25}$, $\gamma = \frac{\pi}{2.25}$ in radians and we use the complex equation for calculating the ψ angle. Inverse kinematic results were $\phi \approx 0.556$ and $\psi \approx 0.796 + i6.287\text{e-}17$. We take the real part of ψ. Rotated $\hat{p}$ and $\hat{l}$ were identical and no error was calculated. Simulations show that for $0 < \varepsilon << 1$ (for the simulation code using Sympy it's been observed that $\varepsilon \approx 1\text{e-}9$):

$$||\hat{l}\cdot\hat{x}|| < 1-\varepsilon \tag{23}$$

$$\rightarrow\ \hat{l}\cdot(\hat{R}_{\hat{x}}(\psi)R_{\hat{w}}(\phi)\hat{p}) > 1-\varepsilon \tag{24}$$

Thus for non-singular values the simulation did not show any signs of significant error, as well as for negative elevation values and the zenith. The simulation has been written in Python using Sympy and Matplotlib. And angles produced has been cross checked using Octave.

Conclusion

Using analytical methods, we produced and, through simulations, verified a more general inverse kinematics solution for X-Y pedestals that take into account joint and pointing misalignments. The inverse kinematics equations have a relatively low computational complexity and (if the computing environment supports complex numbers) are robust for out-of-workspace positions.

Acknowledgements

This research has been funded by **Profen Communication Technologies & Services, Inc.** The author is thankful to Mustafa Çelik, Cem Doğan and Kadir Koca for their guidance on X-Y pedestals, to Merve Güvenç for the inspiring conversations and to Rızkı Tekay for being the catalyst for this research.

References

[1] Tongbo Ji et al. "Analysis of tracking performance for altitude-azimuth pedestal near the zenith". In: *Fifth International Symposium on Instrumentation and Control Technology.* Ed. by Guangjun Zhang, Huijie Zhao, and Zhongyu Wang. Vol. 5253. International Society for Optics and Photonics. SPIE, 2003, pp. 398–401. DOI: 10.1117/12.521401. URL: https://doi.org/10.1117/12.521401.

[2] Daniel H Gottlieb. "Robots and fibre bundles". In: *Bull. Soc. Math. Belg* 38 (1986), pp. 219–223.

[3] Keith Willey. "Selecting a pedestal for tracking LEO satellites at Ka band". In: *Microwave journal* 43.4 (2000), pp. 118–118.

[4] Nafiseh Mazaheri Tehrani et al. "Full extracting kinematic and dynamic equations of X/Y pedestal with velocity analysis". In: *2014 CACS International Automatic Control Conference (CACS 2014).* 2014, pp. 215–221. DOI: 10.1109/CACS.2014.7097190.

[5] Oguz Kaan Hancioglu, Mustafa Celik, and Ugur Tumerdem. "Kinematics and Tracking Control of a Four Axis Antenna for Satcom on the Move". In: *2018 International Power Electronics Conference (IPEC-Niigata 2018 - ECCE Asia).* 2018, pp. 1680–1686. DOI: 10.23919/IPEC.2018.8507963.

[6] E.D. Pohl and H. Lipkin. "Kinematics of complex joint angles in robotics". In: *Proceedings., IEEE International Conference on Robotics and Automation.* 1990, 86–91 vol.1. DOI: 10.1109/ROBOT.1990.125951.